JOURNAL OF APPLIED PHYSICS **107**, 093514 (2010)

Enhancing magnetoelectric effect via the curvature of composite cylinder

H. M. Wang,[1] E. Pan,[2,a)] and W. Q. Chen[1]
[1]*Department of Engineering Mechanics, Zhejiang University, Hangzhou 310027, People's Republic of China*
[2]*Computer Modeling and Simulation Group, University of Akron, Akron, Ohio 44325, USA*

(Received 22 March 2010; accepted 27 March 2010; published online 4 May 2010)

We solved analytically the magnetoelectric (ME) effect in a bilayered piezoelectric/piezomagnetic cylinder under harmonic excitation. We revealed that at a fixed thickness ratio of the layers, the static or low-frequency ME effect can be substantially enhanced by increasing the curvature of the cylinder. In the megahertz frequency domain, on the other hand, we observed that the peak ME effect can be considerably increased by decreasing the curvature. We further showed that at a fixed curvature, the ME effect can be tuned to be around the resonant frequency for giant output by varying the boundary condition and thickness ratio. © *2010 American Institute of Physics*. [doi:10.1063/1.3415528]

I. INTRODUCTION

The magnetoelectric (ME) effect is characterized by the appearance of a polarization (magnetization) in the multiferroic material/composite upon applying a magnetic (electric) field. As the ME coupling could be directly applied to the design of various microwave devices, research in multiferroic materials/composites has attracted broad attentions in recent years, with the focus on enhancing the ME effect. Since single-phase multiferroic materials exhibit only very weak ME effect, research is now switched to the corresponding composites. There are a couple of avenues to increase the ME effect in multiferroic composites: The ME effect could be analyzed from the *ab initio* calculations. This includes the investigation of single-phase materials for the largest possible polarization or magnetization,[1–4] and the interface design for possible large magnetism, such as at the $Fe/BaTiO_3$ and $Fe_3O_4/BaTiO_3(001)$.[5,6] The micromechanics approach can be also applied to investigate the ME effect in multiferroic composites. For instance, it was recently showed that the ME effect could be substantially enhanced if one can properly grade the material property of the composite[7,8] or by varying the mechanical boundary conditions.[9,10] Enhancement of ME effect via possible size-dependent material properties in nanocomposites[11] and via strain tuning in thin films[12] were further reported recently.

In the ME effect studies discussed above, the multiferroic composites were assumed to be in a horizontally layered plate shape. Would the curvature of a multiferroic composite affect the ME coupling? While some experimental analyses were carried out using composite cylinders[13–17] with some interesting observations, there is no rigorous study on the importance of the curvature. Thus, by deriving an exact-closed form solution for a bilayered composite cylinder, this article proves that the ME effect can be tuned and enhanced by the curvature of the cylinder.

a)Electronic mail: pan2@uakron.edu.

II. BASIC EQUATIONS

We consider a piezoelectric (PE)/piezomagnetic (PM) composite cylinder as shown in Fig. 1. The inner layer is piezomagnetic and the outer is piezoelectric. The piezoelectric layer is polarized in the radial direction and is coated with electrodes. The radii of the inner surface, interface, and outer surface are denoted, respectively, by a, b, and c. We assume that the PE/PM composite cylinder is driven by a time-harmonic uniform radial magnetic field $H_r = H_0 \exp(\mathrm{i}\omega t)$ in the PM layer, where H_0 is the given amplitude, $\mathrm{i}=\sqrt{-1}$ the imaginary unit, and ω is the driving circular frequency. For a long composite cylinder its deformation can be described by the polar coordinate system (r,θ). Since for the harmonic motion, all the fields have the same time dependence $\exp(\mathrm{i}\omega t)$, this factor will be dropped in the analysis. Based on the three-dimensional theory of magnetoelectroelastic media,[18,19] the governing equations for PE layer under axisymmetric deformation can be simplified to (under plane-strain deformation), as follows:

$$\sigma_{\theta\theta} = c_{11}\frac{u_r}{r} + c_{13}\frac{du_r}{dr} - e_{31}E_r,$$

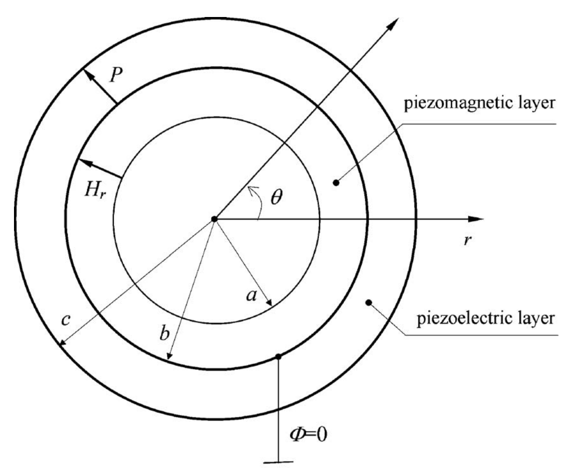

FIG. 1. Schematic of bilayer multiferroic cylindrical structure.

0021-8979/2010/107(9)/093514/4/$30.00

$$\sigma_{rr} = c_{13}\frac{u_r}{r} + c_{33}\frac{du_r}{dr} - e_{33}E_r, \tag{1}$$

$$D_r = e_{31}\frac{u_r}{r} + e_{33}\frac{du_r}{dr} + \varepsilon_{33}E_r,$$

$$\frac{d\sigma_{rr}}{dr} + \frac{\sigma_{rr} - \sigma_{\theta\theta}}{r} + \rho\omega^2 u_r = 0, \tag{2}$$

$$\frac{1}{r}\frac{d}{dr}(rD_r) = 0, \tag{3}$$

$$E_r = -\frac{d\Phi}{dr}, \tag{4}$$

where u_r is the radial displacement and Φ the electric potential; σ_{rr} and $\sigma_{\theta\theta}$ are the radial and hoop stresses; D_r and E_r are the electric displacement and electric field; c_{ij}, e_{3j} and ε_{33} are, respectively, the elastic, piezoelectric, and dielectric coefficients; and ρ is the mass density of the PE material. Similar governing equations can be written for the PM layer[18,19] with Ψ being the magnetic potential; B_r and H_r $[=H_0\exp(i\omega t)]$ the magnetic induction and magnetic field; and q_{3j} and μ_{33} the piezomagnetic and magnetic coefficients.

III. SOLUTIONS OF THE BOUNDARY VALUE PROBLEM, AND THE ME EFFECT

For the bilayered cylinder, we assume that the PE layer is free of charge at its outer boundary $D_r|_{r=c}=0$, and thus $D_r=0$ in the PE layer. Then the third equation of (1) can be rewritten as

$$E_r = -e_{1D}\frac{u_r}{r} - e_{3D}\frac{du_r}{dr}, \tag{5}$$

where $e_{1D}=e_{31}/\varepsilon_{33}$ and $e_{3D}=e_{33}/\varepsilon_{33}$. Substituting Eq. (5) into the first two equations of (1), gives

$$\sigma_{\theta\theta} = c_{1D}\frac{u_r}{r} + c_{3D}\frac{du_r}{dr},$$

$$\sigma_{rr} = c_{3D}\frac{u_r}{r} + c_{0D}\frac{du_r}{dr}, \tag{6}$$

where

$$c_{0D} = c_{33} + e_{33}e_{3D}, \quad c_{1D} = c_{11} + e_{31}e_{1D},$$

$$c_{3D} = c_{13} + e_{31}e_{3D}. \tag{7}$$

Utilizing Eq. (6), Eq. (2) can be rewritten as

$$\frac{d^2u_r}{dr^2} + \frac{1}{r}\frac{du_r}{dr} + \left(k_E^2 - \frac{\mu_E^2}{r^2}\right)u_r = 0, \tag{8}$$

where

$$k_E^2 = \rho\omega^2/c_{0D}, \quad \mu_E^2 = c_{1D}/c_{0D}. \tag{9}$$

The general solution of Eq. (8) is

$$u_r = A_E J_{\mu_E}(k_E r) + B_E Y_{\mu_E}(k_E r). \tag{10}$$

where A_E and B_E are two coefficients to be determined, and $J_\mu(\bullet)$ and $Y_\mu(\bullet)$ are the first and second kind Bessel functions of order μ_E. Similarly, the governing equation for the PM layer can be reduced to

$$\frac{d^2u_r}{dr^2} + \frac{1}{r}\frac{du_r}{dr} + \left(k_M^2 - \frac{\mu_M^2}{r^2}\right)u_r = H_0 Q\frac{1}{r}, \tag{11}$$

where

$$k_M^2 = \frac{\rho\omega^2}{c_{33}}, \quad \mu_M^2 = \frac{c_{11}}{c_{33}}, \quad Q = \frac{q_{33} - q_{31}}{c_{33}}. \tag{12}$$

The general solution of Eq. (11) can be obtained as

$$u_r = A_M J_{\mu_M}(k_M r) + B_M Y_{\mu_M}(k_M r) + H_0 G(r). \tag{13}$$

where A_M and B_M are two undetermined coefficients and

$$G(r) = Q\frac{\pi}{2}\left[Y_{\mu_M}(k_M r)\int_a^r J_{\mu_M}(k_M\xi)d\xi - J_{\mu_M}(k_M r)\int_a^r Y_{\mu_M}(k_M\xi)d\xi\right] = QS_{0,\mu_M}(k_M r), \tag{14}$$

where $S_{0,\mu_M}(k_M r)$ is the Lommel function. If the driving frequency $\omega=0$ (or close to zero), we then have $k_E=0$ for the PE layer and $k_M=0$ for PM layer. Thus solutions for the static (or low-frequency) case can be reduced from Eqs. (10) and (13).

We consider four sets of mechanical boundary conditions (MBCs): (I) Both the inner and outer surfaces are traction free (F-F) $\sigma_{rr}(a)=\sigma_{rr}(c)=0$; (II) The inner surface is clamped while the outer surface is traction free (C-F) $u_r(a)=\sigma_{rr}(c)=0$; (III) The inner surface is traction free while the outer surface is clamped (F-C) $\sigma_{rr}(a)=u_r(c)=0$; and (IV) Both the inner and outer are clamped (C-C) $u_r(a)=u_r(c)=0$. For given MBCs, along with the continuity conditions at the interface, the four unknowns A_E, B_E, A_M, and B_M can be determined. To calculate the ME effect, the average electric field in the piezoelectric layer is adopted. Integrating Eq. (4) over the spatial interval $[b,c]$, employing Eq. (5), and using the inner surface of the PE layer as reference (i.e., we assume that this surface is electrically shorted $\Phi|_{r=b}=0$), then the voltage difference between the inner and outer surfaces of the PE layer can be determined as

$$\Phi_{bc} = e_{3D}[u_r(c) - u_r(b)] + e_{1D}\int_b^c r^{-1}u_r(r)dr. \tag{15}$$

The ME effect is therefore calculated as[1]

$$\alpha = \frac{\Phi_{bc}}{(c-b)H_0}. \tag{16}$$

In our numerical studies, the PM material used is $CoFe_2O_4$ and the PE is PZT-5A.[20] Two dimensionless quantities are introduced in our analysis: One is the thickness ratio m defined as $m=h_E/(h_E+h_M)$, with h_E and h_M being, respectively, the thicknesses of PE and PM layers. The other is the ratio of inner radius to total thickness $R=a/(h_E+h_M)$.

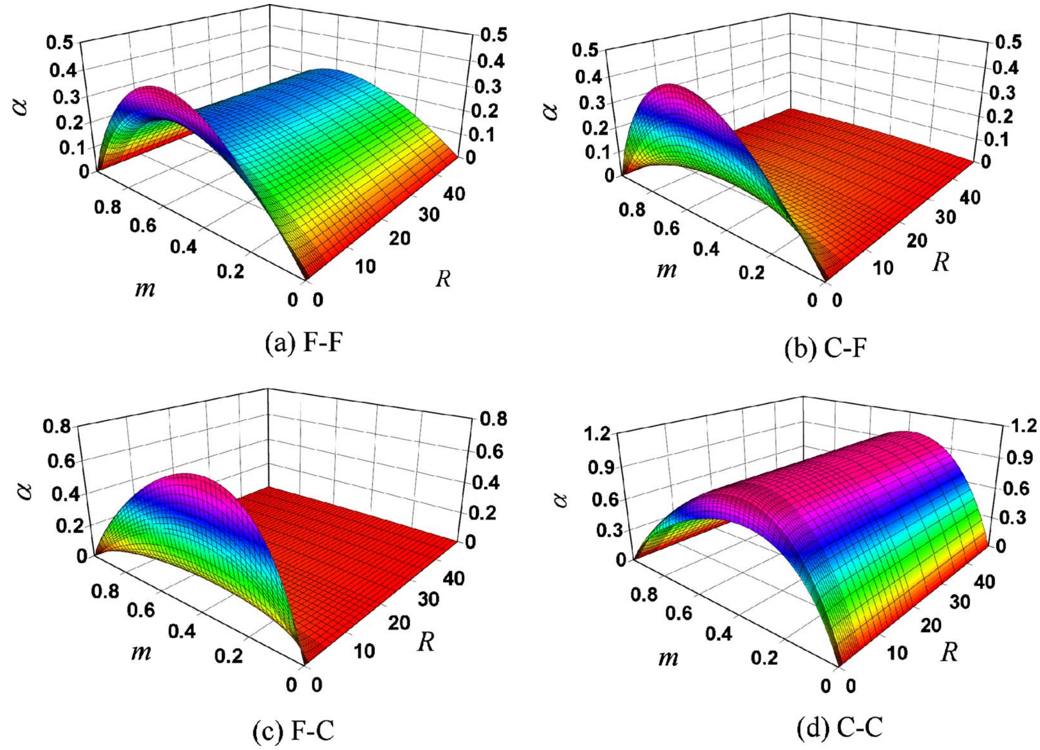

FIG. 2. (Color online) Variation of ME effect α vs m and R for four different boundary conditions (a) F-F; (b) C-F; (c) F-C; (d) C-C. The unit of α is $(\mathrm{V/m})(\mathrm{A/m})^{-1}$.

IV. NUMERICAL RESULTS OF THE ME EFFECT

The ME effect for static or low-frequency case ($\omega \approx 0$) is first investigated. The total thickness of the composite cylinder is 2 mm. Figure 2 shows the three-dimensional variation of the ME effect with respect to m and R for the four different MBCs, and some important features can be observed from it: (1) The ME effect for the clamped MBC (C-C) is much large than that for the other MBCs. This is consistent with previous reports.[9,10] (2) The ME effect can be greatly enhanced by increasing the curvature of the cylinder (or decreasing the radius R). This is particularly true when at least one of the boundaries is traction free (F-F, F-C, or C-F). In other words, at large R, the ME effect could be very weak for MBCs with traction free; however, a relatively strong ME effect can be obtained for small R. (3) The large ME effect corresponding to the C-C MBCs is relatively insensitive to the curvature of the cylinder.

We next consider the ME effect for harmonic driving case in the megahertz (MHz) frequency domain. In the calculation, the elastic constants of PE and PM layers are multiplied by a complex factor $(1+0.05i)$ for viscous damping.[21] Such a treatment has two advantages: (1) with the introduced damping, numerical singularity at the resonant frequency can be avoided; (2) it is practical to take account of the energy dissipation in real materials. In this example, the thickness of the PE and PM layers are both equal 1 mm (i.e., for fixed thickness ratio of the composite cylinder $m=0.5$). Figure 3 shows the variation of ME effect in the bilayered cylinder with different geometric size under different driving frequencies. It is observed clearly that for the four different sets of MBCs, large ME effect is obtained when the composites are driven at the resonant frequency, as was also reported for multiferroic composites with other configurations.[15,22] This is due to the fact that the resonant frequency can cause a stronger mechanical interaction between PE and PM layers. We also notice that the MBCs and the radius of the cylinder have significant effect on the resonant frequency and, hence, on the induced ME effect in the composite cylinder. It is par-

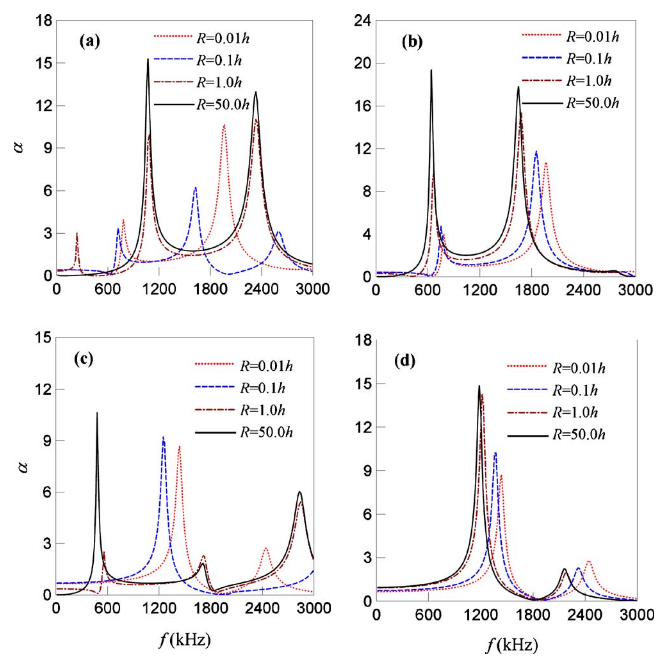

FIG. 3. (Color online) Variation of ME effect α vs driving frequency for four different boundary conditions and different radii of the cylinder. (a) F-F; (b) C-F; (c) F-C; (d) C-C. The unit of α is $(\mathrm{V/m})(\mathrm{A/m})^{-1}$.

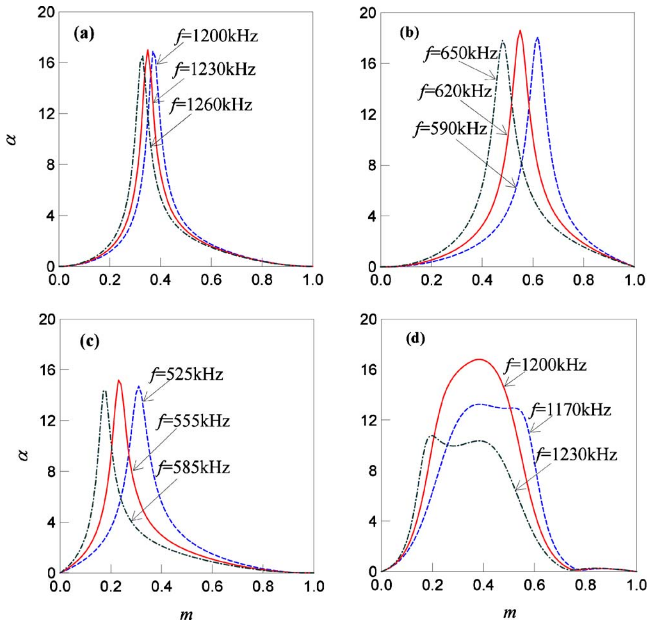

FIG. 4. (Color online) Variation of ME effect α vs the thickness ratio m for four different boundary conditions and different driving frequencies. (a) F-F; (b) C-F; (c) F-C; (d) C-C. The unit of α is $(V/m)(A/m)^{-1}$.

ticularly interesting, as opposite to the static (or low-frequency) case, that in the MHz frequency domain, the ME effect can be increased by decreasing the curvature (i.e., increasing R). In other words, one should make the composite cylinder with a large radius in order to enhance the peak ME effect in the MHz frequency domain.

Finally, at the fixed curvature (or fixed R), we study the variation of the ME effect with the thickness ratio m for three driving frequencies under the four sets of MBCs. For each MBCs, the middle driving frequency corresponds to the one at which the maximum ME effect can be reached. The other two driving frequencies are obtained by a 30 kHz shift. Figure 4 shows that for a given MBC, the thickness ratio m corresponding to the maximum ME effect can be different for different driving frequencies. For instance, for the C-F MBC, the maximum ME effect for $f=620$ kHz is reached at $m=0.55$, for $f=590$ kHz at $m=0.62$, and for $f=650$ kHz at $m=0.48$ [Fig. 4(b)]. This figure shows clearly that at a fixed curvature and for a given driving frequency, one can still tune the ME effect to its maximum by varying the MBC and/or the thickness ratio of the composite cylinder.

V. CONCLUSIONS

In conclusion, we have derived an analytical solution for the ME effect in a bilayered piezoelectric/piezomagnetic cylinder. Our results show that at a fixed thickness ratio of the layers, the static or low-frequency ME effect can be substantially enhanced by increasing the curvature of the cylinder, particularly for the boundary condition case involving traction free. This interesting feature is consistent with recent observations.[13,14] On the other hand, in the MHz frequency domain, the peak ME effect can be considerably intensified by decreasing its curvature. We further show that for a fixed curvature, the ME effect can be adjusted to be around the resonant frequencies (so that it has a maximum output) by varying the MBC and thickness ratio of the composite cylinder. In other words, giant ME coupling effect at a given resonant frequency can be achieved by tuning the MBC and thickness ratio of the composite cylinder.

ACKNOWLEDGMENTS

The work was supported by the National Natural Science Foundation of China (Grant Nos. 10872179, 10725210, and 10832009), the Zhejiang Provincial Natural Science Foundation of China (Grant No. Y7080298), and the Zijin and Xinxing Plans of Zhejiang University. It was also partially supported by AFOSR under Grant No. FA9550-06-1-0317.

[1] M. Fiebig, J. Phys. D **38**, R123 (2005).
[2] P. Baettig and N. A. Spaldin, Appl. Phys. Lett. **86**, 012505 (2005).
[3] W. Eerenstein, N. D. Mathur, and J. F. Scott, Nature (London) **442**, 759 (2006).
[4] C. W. Nan, M. I. Bichurin, S. X. Dong, D. Viehland, and G. Srinivasan, J. Appl. Phys. **103**, 031101 (2008).
[5] C. G. Duan, S. S. Jaswal, and E. Y. Tsymbal, Phys. Rev. Lett. **97**, 047201 (2006).
[6] M. K. Niranjan, J. P. Velev, C. G. Guan, S. S. Jaswal, and E. Y. Tsymbal, Phys. Rev. B **78**, 104405 (2008).
[7] V. M. Petrov and G. Srinivasan, Phys. Rev. B **78**, 184421 (2008).
[8] X. Wang, E. Pan, J. D. Albrecht, and W. J. Feng, Compos. Struct. **87**, 206 (2009).
[9] M. I. Bichurin, V. M. Petrov, and G. Srinivasan, Phys. Rev. B **68**, 054402 (2003).
[10] E. Pan and R. Wang, J. Phys. D **42**, 245503 (2009).
[11] E. Pan, X. Wang, and R. Wang, Appl. Phys. Lett. **95**, 181904 (2009).
[12] X. Marti, I. Fina, V. Skumryev, C. Ferrater, M. Varela, L. Fabrega, F. Sanchez, and J. Fontcuberta, Appl. Phys. Lett. **95**, 142903 (2009).
[13] M. I. Bichurin, D. Viehland, and G. Srinivasan, J. Electroceram. **19**, 243 (2007).
[14] V. M. Petrov, G. Srinivasan, M. I. Bichurin, and A. Gupta, Phys. Rev. B **75**, 224407 (2007).
[15] C. L. Zhang, J. S. Yang, and W. Q. Chen, Int. J. Appl. Electromagn. Mech. **28**, 441 (2008).
[16] D. A. Pan, Y. Bai, A. A. Volinsky, W. Y. Chu, and L. J. Qiao, Appl. Phys. Lett. **92**, 052904 (2008).
[17] C. L. Zhang, W. Q. Chen, S. H. Xie, J. S. Yang, and J. Y. Li, Appl. Phys. Lett. **94**, 102907 (2009).
[18] E. Pan, J. Appl. Mech. **68**, 608 (2001).
[19] P. F. Hou and A. Y. T. Leung, Smart Mater. Struct. **13**, 762 (2004).
[20] F. Ramirez, P. R. Heyliger, and E. Pan, J. Sound Vib. **292**, 626 (2006).
[21] C. L. Zhang, W. Q. Chen, J. Y. Li, and J. S. Yang, Smart Mater. Struct. **18**, 095026 (2009).
[22] M. I. Bichurin, D. A. Filippov, V. M. Petrov, V. M. Laletsin, N. Paddubnaya, and G. Srinivasan, Phys. Rev. B **68**, 132408 (2003).